Available online at www.sciencedirect.com
ScienceDirect
Bioorganic & Medicinal Chemistry 14 (2006) 8210–8218
Bioorganic & Medicinal Chemistry

Probing the physicochemical and structural requirements for glycogen synthase kinase-3α inhibition: 2D-QSAR for 3-anilino-4-phenylmaleimides

Prasanna Sivaprakasam,[a] Aihua Xie[a] and Robert J. Doerksen[a,b,*]

[a]*Department of Medicinal Chemistry, School of Pharmacy, University of Mississippi, MS 38677-1848, USA*
[b]*Research Institute for Pharmaceutical Sciences, School of Pharmacy, University of Mississippi, MS 38677-1848, USA*

Received 14 July 2006; revised 12 September 2006; accepted 12 September 2006
Available online 28 September 2006

Abstract—Glycogen synthase kinase-3α (GSK-3α) was recently found to be an attractive target for the treatment of Alzheimer's disease due to its dual action in the formation of both amyloid plaques and neurofibrillary tangles. It is also a viable target for many other diseases, such as type 2 diabetes. Reported herein is a 2D-QSAR exploration of the physicochemical (hydrophobic, electronic, and steric) and structural requirements among 3-anilino-4-phenylmaleimides toward GSK-3α binding. Using Fujita–Ban and Hansch QSAR analysis, electronic and steric interactions at the 4-phenyl ring and hydrophobic interactions at the 3-anilino ring are shown to be crucial. Analysis of the 4-phenyl ring of these compounds using common aromatic substituent constants showed electron-withdrawing and bulky *ortho* substituents as imperative for GSK-3α inhibition.

1. Introduction

Glycogen synthase kinase-3 (GSK-3) is a serine/threonine kinase that phosphorylates glycogen synthase in the rate-limiting step of glycogen biosynthesis.[1] GSK-3, which belongs to the special class of mitogen activated protein (MAP) kinases,[2] was identified in 1980.[3] Considerable interest has developed in GSK-3 due to its potential as a target to regulate blood glucose levels by different mechanisms[4–8] which could be used to treat type 2 diabetes[7,8] and to its implication in Alzheimer's disease.[9–12] GSK-3 is also a potential target for the treatment of stroke,[13] cancer,[14] bipolar disorder,[15] and malaria, for which a recent investigation by Droucheau et al.[16] showed that there is potential to be able to design selective inhibitors of *Plasmodium falciparum* GSK-3.

Three isoforms of GSK-3 have been identified in mammalian cells, GSK-3α, GSK-3β, and GSK-3β2 (a splicing variant of GSK-3β).[9,17,18] The α and β isoforms show a substantial deviation in protein sequence, mostly outside the kinase core (308 residues), but the core has 97% sequence similarity and overall 91% identity.[1] Both isoforms have been implicated in the formation of neurofibrillary tangles.[9,11] Even though the α and β forms are 97% identical with respect to their kinase domain, studies performed by Phiel et al.[9] showed that selective reduction in concentration of the α isoform led to a decrease in the concentration of $A\beta_{40}$ and $A\beta_{42}$, primary constituents of amyloid plaques in Alzheimer's disease (AD), whereas decreased expression of the β isoform led to a slight increase in the concentration of the two Aβ peptides. Thus inhibition of GSK-3α could potentially provide dual therapy against AD, preventing the buildup of amyloid plaques and of neurofibrillary tangles.[9,11] We have begun a research effort to study compounds showing inhibition against GSK-3α and to derive as much information as possible regarding their binding mode as a starting point toward development of a selective inhibitor for this target.

Since 1998 there have been many reports of GSK-3 inhibitors.[19–30] In this work we consider maleimides which were some of the first inhibitors to be reported as selectively active against GSK-3.[20,21] Researchers from SmithKline Beecham focused on GSK-3α and discovered the maleimide inhibitors through high throughput screening of the SmithKline Beecham compound

Keywords: GSK-3; Maleimides; Phosphorylation; QSAR; Transferases.
* Corresponding author. Tel.: +1 662 915 5880; fax: +1 662 915 5638; e-mail: rjd@olemiss.edu

0968-0896/$ - see front matter © 2006 Elsevier Ltd. All rights reserved.
doi:10.1016/j.bmc.2006.09.021

collection.[20,21] They used in vitro binding to rabbit GSK-3α, which shows 95% homology to human GSK-3α and is >99% identical in the kinase domain,[21] and synthesized several analogues, some of which were potent and selective.[21]

Herein, we report a 2D-QSAR (quantitative structure–activity relationship) study to rationalize the physicochemical and structural features among the reported 3-anilino-4-phenylmaleimides.[21] Since the seminal work of Hansch 40 years ago,[31] quantitative structure–activity relationship (QSAR) research has been considered a major tool in drug discovery to explore ligand–receptor/enzyme interactions, especially when the structural details of the target are not known.[32] For GSK-3, it is important to note that X-ray structures are available for GSK-3β[33,34] but not for GSK-3α, though the isoforms are highly homologous. QSAR is an effective way of optimizing or correlating the biological activity within a congeneric series with certain structural features or with atomic, group or molecular descriptors, such as lipophilicity, polarizability, or electronic and steric properties. The diverse structural variation in the maleimide data set (nature and size of substituents) encouraged us to perform a Fujita–Ban approach,[35] which is well suited for the present case. However, in order to derive meaningful physicochemical requirements and to probe the mechanistic aspects of putative ligand–GSK-3α enzyme interactions, we also adopted Hansch QSAR analysis. In spite of the spectacular development of modern computational tools in the area of QSAR research, Hansch type QSAR is still widely used in the lead optimization stage of synthetic and other projects.[32] This method continues to provide valuable insights about ligand–enzyme interactions and challenges more computationally intensive 3D-QSAR approaches such as CoMFA and CoMSIA,[36,37] with major strengths being that alignment of the ligands is unnecessary (avoiding the assumption that all ligands bind in the same pose), the variety of descriptors which can be employed, and ease of interpretability. Some computational analysis of GSK-3 inhibitors has been reported including QSAR and other molecular modeling studies on β isoforms.[30,38–43] Two reports[39,42] which included the maleimides of Smith et al.[21] will be discussed below.

2. Results and discussion

The aromatic substituent constants and indicator variables used in the present study are listed in Table 1. Fujita–Ban models are given in Table 2. Hansch QSAR models are presented in Table 3. In the Tables, numbers given in parentheses following the coefficient terms are the standard error of the regression terms and of the constant for a QSAR.

2.1. Fujita–Ban analysis

For Fujita–Ban type analysis, the observed GSK-3α inhibitory activity was considered as the dependent variable and the indicator variables as independent variables. At any given position in either ring of the maleimides, the frequency of occurrence of each substituent is more than one. This enabled us to start the Fujita–Ban analysis with **1** (R = R_1 = H) as the parent structure. All the independent structural variables were fitted to a multiple linear regression equation, resulting in QSAR Model 0a which has excellent statistical parameters for the set of 64 compounds: $r = 0.938$, $r^2 = 0.880$, $s = 0.144$, and $F = 21.52$. The Fujita–Ban contribution of each substituent is given in Table 2. Only 10 of the 16 structural variables were found to be significant above the 95% confidence interval. We then used stepwise linear regression to obtain the more compact QSAR Model 0b (cf. Table 2), with $n = 64$, $r^2 = 0.845$, $s = 0.152$, and $F = 32.71$, using only 9 variables. For Model 0b compared to Model 0a, r^2 is slightly lower but F is considerably higher. The high r^2 and F of the models provide an affirmation of the worth of Fujita–Ban analysis for the present study. From Model 0a, it is evident that substituents 2-Cl, 3-Cl, 4-Cl, 2-OCH_3, 3-OCH_3, 4-OCH_3, 2-NO_2, 3-NO_2, and 4-NO_2 at the 4-phenyl ring are positively correlated with GSK-3α inhibitory activity. Similarly, substituents such as 3-Cl, 4-Cl, 5-Cl, 3-COOH, 4-OH, and 4-SCH_3 at the 3-anilino ring are positively and 3-OH is negatively correlated with GSK-3α inhibitory activity. According to both models, 3-NO_2 and 2-NO_2 contribute to the activity the most.

2.2. Hansch 2D-QSAR

Any conclusions derived from the Fujita–Ban model are only applicable to the range of substituents used in the analysis, so in order to provide more generalized and meaningful insight into the physicochemical role of the substituents, we chose next to perform a Hansch type QSAR study. Here, the observed GSK-3α inhibitory activity was the dependent variable and calculated physicochemical properties and indicator variables served as the independent variables while performing forward-stepping regression. The statistically significant QSAR models we found are given in Table 3 and the accompanying statistical parameters used to evaluate them are in Table 4. QSAR Models 1–3 were developed for the set of 64 3-anilino-4-phenyl derivatives. These models clearly show that apart from the physicochemical requirements at the 4-phenyl ring (R substituents in Table 1) some structural features at the anilino ring (R_1 substituents) are also essential for GSK-3α inhibitory activity. The indicator variables used in Model 1, I_{3ClR1}, I_{4ClR1}, and I_{3OHR1}, denote the presence or absence of 3-Cl, 4-Cl, and 3-OH groups, respectively, at R_1. The positive coefficients of I_{3ClR1} and I_{4ClR1} suggest that 3- and 4-chloro substitution at the anilino ring enhances activity. The negative coefficient of I_{3OHR1} shows that a hydroxyl substitution at the 3-position of R_1 is detrimental to GSK-3α inhibitory activity. The positive contribution of the electronic parameter, σ_{metaR}, suggests that electron-withdrawing groups at the *meta* position of R are crucial for GSK-3α inhibitory activity. The positive contribution of the descriptor HA_R indicates that hydrogen bonding interactions between acceptor probes such as methoxy or nitro groups of R and the complementary donor groups of the amino acids at the binding site of the GSK-3α enzyme are important. The squared

Table 1. 3-Anilino-4-phenylmaleimides observed and converted activities, aromatic substituent constants, and indicator variables used in 2D-QSAR models

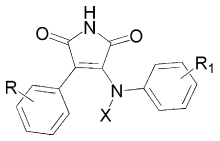

Compound	R	R_1	X	IC_{50}[a]	pIC_{50}[b]	HA_R	f_{ortho}	σ_{metaR}	I_{3ClR1}	I_{4ClR1}	I_{3OHR1}	I_{xCH3}	E^s_{orthoR}	π_{metaR1}
1	H	H	H	529	6.28	0	0	0	0	0	0	0	0	0
2	2-Cl	H	H	216	6.67	0	0.41	0	0	0	0	0	−0.97	0
3	2-OCH_3	H	H	216	6.67	1	0.26	0	0	0	0	0	−0.55	0
4	3-NO_2	H	H	141	6.85	1	0	0.71	0	0	0	0	0	0
5	4-Cl	H	H	514	6.29	0	0	0	0	0	0	0	0	0
6	4-OCH_3	H	H	390	6.41	1	0	0	0	0	0	0	0	0
7	H	3-Cl	H	301	6.52	0	0	0	1	0	0	0	0	0.71
8	2-Cl	3-Cl	H	195	6.71	0	0.41	0	1	0	0	0	−0.97	0.71
9	2-OCH_3	3-Cl	H	114	6.94	1	0.26	0	1	0	0	0	−0.55	0.71
10	2-NO_2	3-Cl	H	104	6.98	1	0.67	0	1	0	0	0	−1.01	0.71
11	3-OCH_3	3-Cl	H	257	6.59	1	0	0.12	1	0	0	0	0	0.71
12	3-NO_2	3-Cl	H	70	7.15	1	0	0.71	1	0	0	0	0	0.71
13	4-Cl	3-Cl	H	447	6.35	0	0	0	1	0	0	0	0	0.71
14	4-OCH_3	3-Cl	H	156	6.81	1	0	0	1	0	0	0	0	0.71
15	H	3-OH	H	704	6.15	0	0	0	0	0	1	0	0	−0.67
16	2-Cl	3-OH	H	374	6.43	0	0.41	0	0	0	1	0	−0.97	−0.67
17	2-OCH_3	3-OH	H	259	6.59	1	0.26	0	0	0	1	0	−0.55	−0.67
18	2-NO_2	3-OH	H	251	6.60	1	0.67	0	0	0	1	0	−1.01	−0.67
19	3-Cl	3-OH	H	1478	5.83	0	0	0.37	0	0	1	0	0	−0.67
20	3-OCH_3	3-OH	H	472	6.33	1	0	0.12	0	0	1	0	0	−0.67
21	3-NO_2	3-OH	H	236	6.63	1	0	0.71	0	0	1	0	0	−0.67
22	4-Cl	3-OH	H	407	6.39	0	0	0	0	0	1	0	0	−0.67
23	4-OCH_3	3-OH	H	481	6.32	1	0	0	0	0	1	0	0	−0.67
24	3-NO_2	4-OH	H	123	6.91	1	0	0.71	0	0	0	0	0	0
25	4-Cl	4-OH	H	317	6.50	0	0	0	0	0	0	0	0	0
26	2-Cl	3-Cl,4-OH	H	152	6.82	0	0.41	0	1	0	0	0	−0.97	0.71
27	2-OCH_3	3-Cl,4-OH	H	139	6.86	1	0.26	0	1	0	0	0	−0.55	0.71
28	2-NO_2	3-Cl,4-OH	H	104	6.98	1	0.67	0	1	0	0	0	−1.01	0.71
29	3-Cl	3-Cl,4-OH	H	94	7.03	0	0	0.37	1	0	0	0	0	0.71
30	3-NO_2	3-Cl,4-OH	H	59	7.23	1	0	0.71	1	0	0	0	0	0.71
31	4-Cl	3-Cl,4-OH	H	173	6.76	0	0	0	1	0	0	0	0	0.71
32	H	3,5-di-Cl,4-OH	H	149	6.83	0	0	0	1	0	0	0	0	1.42
33	2-Cl	3,5-di-Cl,4-OH	H	93	7.03	0	0.41	0	1	0	0	0	−0.97	1.42
34	2-OCH_3	3,5-di-Cl,4-OH	H	82	7.09	1	0.26	0	1	0	0	0	−0.55	1.42
35	2-NO_2	3,5-di-Cl,4-OH	H	52	7.28	1	0.67	0	1	0	0	0	−1.01	1.42
36	3-Cl	3,5-di-Cl,4-OH	H	58	7.24	0	0	0.37	1	0	0	0	0	1.42
37	3-OCH_3	3,5-di-Cl,4-OH	H	142	6.85	1	0	0.12	1	0	0	0	0	1.42
38	3-NO_2	3,5-di-Cl,4-OH	H	20	7.70	1	0	0.71	1	0	0	0	0	1.42
39	4-Cl	3,5-di-Cl,4-OH	H	91	7.04	0	0	0	1	0	0	0	0	1.42
40	4-OCH_3	3,5-di-Cl,4-OH	H	83	7.08	1	0	0	1	0	0	0	0	1.42
41	4-NO_2	3,5-di-Cl,4-OH	H	71	7.15	1	0	0	1	0	0	0	0	1.42
42	H	3-COOH	H	291	6.54	0	0	0	0	0	0	0	0	−0.32
43	2-Cl	3-COOH	H	136	6.87	0	0.41	0	0	0	0	0	−0.97	−0.32
44	3-Cl	3-COOH	H	134	6.87	0	0	0.37	0	0	0	0	0	−0.32
45	3-OCH_3	3-COOH	H	195	6.71	1	0	0.12	0	0	0	0	0	−0.32
46	3-NO_2	3-COOH	H	79	7.10	1	0	0.71	0	0	0	0	0	−0.32
47	4-Cl	3-COOH	H	186	6.73	0	0	0	0	0	0	0	0	−0.32
48	4-OCH_3	3-COOH	H	214	6.67	1	0	0	0	0	0	0	0	−0.32
49	H	4-Cl,3-COOH	H	143	6.85	0	0	0	0	1	0	0	0	−0.32
50	2-Cl	4-Cl,3-COOH	H	74	7.13	0	0.41	0	0	1	0	0	−0.97	−0.32
51	2-NO_2	4-Cl,3-COOH	H	28	7.55	1	0.67	0	0	1	0	0	−1.01	−0.32
52	3-Cl	4-Cl,3-COOH	H	76	7.12	0	0	0.37	0	1	0	0	0	−0.32
53	3-OCH_3	4-Cl,3-COOH	H	85	7.07	1	0	0.12	0	1	0	0	0	−0.32
54	3-NO_2	4-Cl,3-COOH	H	26	7.59	1	0	0.71	0	1	0	0	0	−0.32
55	4-Cl	4-Cl,3-COOH	H	109	6.96	0	0	0	0	1	0	0	0	−0.32
56	H	4-SCH_3	H	404	6.39	0	0	0	0	0	0	0	0	0
57	2-Cl	4-SCH_3	H	161	6.79	0	0.41	0	0	0	0	0	−0.97	0

Table 1 (*continued*)

Compound	R	R_1	X	IC_{50}[a]	pIC_{50}[b]	HA_R	f_{ortho}	σ_{metaR}	I_{3ClR1}	I_{4ClR1}	I_{3OHR1}	I_{xCH3}	E^s_{orthoR}	π_{metaR1}
58	2-OCH_3	4-SCH_3	H	110	6.96	1	0.26	0	0	0	0	0	−0.55	0
59	3-Cl	4-SCH_3	H	532	6.27	0	0	0.37	0	0	0	0	0	0
60	3-OCH_3	4-SCH_3	H	203	6.69	1	0	0.12	0	0	0	0	0	0
61	3-NO_2	4-SCH_3	H	152	6.82	1	0	0.71	0	0	0	0	0	0
62	4-Cl	4-SCH_3	H	529	6.28	0	0	0	0	0	0	0	0	0
63	4-OCH_3	4-SCH_3	H	243	6.61	1	0	0	0	0	0	0	0	0
64	4-NO_2	4-SCH_3	H	392	6.41	1	0	0	0	0	0	0	0	0
65	H	H	CH_3	2613	5.58	0	0	0	0	0	0	1	0	0
66	3-NO_2	H	CH_3	1398	5.85	1	0	0.71	0	0	0	1	0	0
67	4-Cl	H	CH_3	2285	5.64	0	0	0	0	0	0	1	0	0

[a] Observed activity (nM).
[b] Converted (log) activity.

Table 2. Fujita–Ban contribution of substituents over 4-phenyl and 3-anilino ring of 3-anilino-4-phenylmaleimides

Substitution	Ring[a]	No.[b]	Model-0a[c]	Model-0b[c]
Parent structure			6.255 (±0.074)	6.436 (±0.041)
2-Cl	R	8	0.286 (±0.075)	0.167 (±0.060)
2-OCH_3	R	6	0.407 (±0.081)	0.285 (±0.068)
3-NO_2	R	9	0.605 (±0.074)	0.492 (±0.057)
3-Cl	R	6	0.157 (±0.081)	—
4-Cl	R	9	0.086 (±0.074)	—
4-OCH_3	R	6	0.212 (±0.080)	—
2-NO_2	R	5	0.485 (±0.086)	0.371 (±0.075)
3-OCH_3	R	5	0.157 (±0.080)	—
4-NO_2	R	2	0.167 (±0.119)	—
3-Cl	R_1	24	0.227 (±0.066)	0.214 (±0.056)
3-OH	R_1	9	−0.159 (±0.073)	−0.220 (±0.063)
4-OH	R_1	18	0.121 (±0.067)	—
5-Cl	R_1	10	0.269 (±0.072)	0.346 (±0.063)
3-COOH	R_1	14	0.315 (±0.078)	0.254 (±0.069)
4-Cl	R_1	7	0.358 (±0.078)	0.344 (±0.082)
4-SCH_3	R_1	9	0.096 (±0.074)	—

[a] The ring to which the substituent is attached, R for 4-phenyl and R_1 for 3-anilino ring, respectively.
[b] Frequency of occurrence of substituent at R or at R_1.
[c] See text for statistical parameters.

correlation coefficient (r^2) and predictability of Model 1 are fairly good; the model explains 66.5% of the variance of the observed GSK-3α inhibitory activity.

Since we found a positive correlation of σ_{orthoR} (data not shown) as of σ_{metaR} with bioactivity, we focused our attention next on the influence of *ortho* substituents on the 4-phenyl ring. According to Fujita and Nishioka[44] and the further investigations by Hansch[45] the role of *ortho* substituents in QSAR can be clarified by testing the compound descriptor $\sigma + f + E^s$, where σ = Hammett electronic substituent constant, f = inductive parameter, and E^s = steric descriptor. Hence, we added the inductive parameter f for *ortho* substituents, namely f_{ortho}, to Model 1 to obtain QSAR Model 2. This improved the correlation (r^2 increased from 0.67 to 0.74). The significance level as reflected by Fischer F also increased. The standard error of estimate decreased and the predictability of the model as reflected by the *loo* cross-validated q^2 increased. Proximity electronic effects can also be well represented by f_{ortho}. The positive correlation of f_{ortho} with activity suggests that inductively electron-withdrawing substituents like nitro, trifluoromethyl, etc., are favorable at the *ortho* R position. Next, we tested the steric descriptor E^s as an additional descriptor. Model 3 included E^s_{orthoR} for *ortho* substituents on the R ring. The correlation is almost the same as for Model 2. Since both electron-withdrawing and -donating *ortho* substituents are found to have similar influence on GSK-3α inhibitory activity (compare **2** and **3**; **9** and **10**; **17** and **18**; **26** and **27**; **33** and **34**), one might expect the *ortho* steric effect to be more important than the electronic effect for improving the GSK-3α inhibitory activity among these congeners. On the contrary, from Models 2 to 3 there was negligible improvement in the correlation coefficient and other statistical parameters. This is not surprising to us: the intercorrelation among pairs of descriptors used in Models 1–3 had an absolute value <0.4 except for f_{ortho} and E^s_{orthoR} which are highly (inversely) correlated, with $r = -0.97$. For this reason, we did not use the two descriptors together in any of our reported QSAR models. Thus both electronic and steric effects of the *ortho* substituents have important influence on the GSK-3α inhibitory activity enhancement among these congeners. The negative contribution of the steric term E^s_{orthoR} suggests that the bulkier the *ortho* substituent at the 4-phenyl ring, the higher is the GSK-3α inhibitory activity. Interestingly, σ_{orthoR} itself gave poorer models than the other *ortho* descriptors, though it is highly correlated with them, with $r = 0.74$ with f_{ortho} and $r = -0.62$ with E^s_{orthoR}.

Models 4–14 were developed for the combined dataset of 64 3-anilino and 3 3-*N*-methyl anilino derivatives (cf. Tables 3 and 4). The use of the indicator variable I_{xCH3} (which = 1 for 3-*N*-methylanilino derivatives and = 0 for 3-anilino derivatives) enabled us to study both groups of compounds together. Models 4–14 indicate that a similar trend in the structural features at both the anilino and *N*-methylanilino rings occurred in the combined analysis. The negative contribution of I_{xCH3} in Model 4 shows that the 3-*N*-methylanilino derivatives are unfavorable for GSK-3α inhibitory activity in comparison to 3-anilino derivatives, as already noted by Smith et al.[21]. Model 5, obtained by adding σ_{metaR} to Model 4, explains 76.2% of the variance in observed GSK-3α inhibitory activity. Models 6 and 7 included f_{ortho} and E^s_{orthoR}, respectively, to test for effects of *ortho* substituents as in Models 2 and 3, above. They were

Table 3. 2D-QSAR models for 3-anilino-4-phenylmaleimides

QSAR model	Regression coefficients									Constant
	HA_R	I_{3ClR1}	I_{4ClR1}	I_{3OHR1}	σ_{metaR}	f_{ortho}	E^{s}_{orthoR}	I_{xCH3}	π_{metaR1}	
1	0.185 (±0.057)	0.318 (±0.063)	0.553 (±0.093)	−0.275 (±0.085)	0.376 (±0.112)	—	—	—	—	6.484 (±0.053)
2	0.147 (±0.051)	0.279 (±0.057)	0.507 (±0.084)	−0.307 (±0.076)	0.540 (±0.107)	0.500 (±0.124)	—	—	—	6.441 (±0.048)
3	0.168 (±0.050)	0.284 (±0.056)	0.518 (±0.083)	−0.301 (±0.075)	0.537 (±0.106)	—	−0.269 (±0.065)	—	—	6.422 (±0.049)
4	0.238 (±0.057)	0.303 (±0.067)	0.561 (±0.099)	−0.288 (±0.090)	—	—	—	−0.904 (±0.142)	—	6.518 (±0.055)
5	0.180 (±0.056)	0.318 (±0.062)	0.553 (±0.092)	−0.275 (±0.084)	0.357 (±0.107)	—	—	−0.942 (±0.132)	—	6.490 (±0.052)
6	0.140 (±0.051)	0.280 (±0.056)	0.508 (±0.083)	−0.306 (±0.075)	0.510 (±0.104)	0.489 (±0.123)	—	−0.924 (±0.118)	—	6.450 (±0.047)
7	0.161 (±0.050)	0.285 (±0.056)	0.519 (±0.082)	−0.300 (±0.075)	0.505 (±0.102)	—	−0.261 (±0.064)	−0.913 (±0.118)	—	6.432 (±0.048)
8	—	—	0.644 (±0.105)	—	—	—	—	−0.947 (±0.150)	0.321 (±0.048)	6.640 (±0.036)
9	0.230 (±0.056)	—	0.664 (±0.094)	—	—	—	—	−0.901 (±0.135)	0.310 (±0.043)	6.518 (±0.044)
10	0.221 (±0.054)	—	0.651 (±0.092)	—	—	0.258 (±0.129)	—	−0.873 (±0.132)	0.303 (±0.042)	6.492 (±0.045)
11	0.232 (±0.054)	—	0.655 (±0.091)	—	—	—	−0.148 (±0.068)	−0.866 (±0.132)	0.304 (±0.042)	6.482 (±0.046)
12	0.169 (±0.054)	—	0.651 (±0.086)	—	0.374 (±0.103)	—	—	−0.947 (±0.124)	0.318 (±0.039)	6.495 (±0.040)
13	0.127 (±0.048)	—	0.621 (±0.076)	—	0.532 (±0.099)	0.492 (±0.116)	—	−0.912 (±0.110)	0.308 (±0.035)	6.437 (±0.038)
13a[a]	0.099 (±0.044)	—	0.593 (±0.070)	—	0.582 (±0.090)	0.495 (±0.105)	—	−0.940 (±0.100)	0.288 (±0.032)	6.462 (±0.035)
14	0.148 (±0.047)	—	0.630 (±0.076)	—	0.527 (±0.097)	—	−0.265 (±0.060)	−0.903 (±0.109)	0.310 (±0.035)	6.421 (±0.039)
14a[a]	0.122 (±0.044)	—	0.602 (±0.069)	—	0.573 (±0.089)	—	−0.262 (±0.055)	−0.930 (±0.099)	0.290 (±0.032)	6.447 (±0.036)

[a] QSAR models obtained without compound **19**.

Table 4. Statistical parameters of 2D-QSAR models for 3-anilino-4-phenylmaleimides

QSAR model	n	r	r^2	F	s	q^2
1	64	0.815	0.665	23.0	0.216	0.590
2	64	0.860	0.739	26.9	0.192	0.675
3	64	0.862	0.743	27.5	0.191	0.679
4	67	0.847	0.718	31.1	0.231	0.671
5	67	0.873	0.762	32.0	0.214	0.706
6	67	0.901	0.812	36.5	0.191	0.761
7	67	0.902	0.814	36.9	0.190	0.762
8	67	0.806	0.650	39.1	0.253	0.608
9	67	0.852	0.726	41.0	0.226	0.688
10	67	0.862	0.743	35.2	0.220	0.702
11	67	0.863	0.745	35.7	0.219	0.705
12	67	0.880	0.774	41.8	0.206	0.732
13	67	0.909	0.827	47.6	0.182	0.788
13a[a]	66	0.922	0.850	55.6	0.165	0.814
14	67	0.911	0.829	48.6	0.181	0.789
14a[a]	66	0.922	0.850	55.9	0.165	0.813

[a] QSAR models obtained without compound **19**.

slightly improved models, capturing over 81% of the variance.

The contribution of the structural features 3-Cl, 4-Cl, and 3-OH at R_1 in all the above QSAR models prompted us to test the anilino ring for any physicochemical significance. Testing of QSAR models containing aromatic substituent constants for the anilino ring resulted in Models 8–14. The initial contribution of $\Sigma\pi_{R1}$ in a QSAR model along with HA_R and I_{xCH3} (model not shown) showed that hydrophobic substituents at the R_1 ring are favorable for GSK-3α inhibitory activity. In order to get more insight about the position-specific hydrophobic requirements on R_1, we used hydrophobic constants for substituents at the *ortho*, *meta*, and *para* positions, labeled $\pi_{orthoR1}$, π_{metaR1}, and π_{paraR1}, respectively. The positive contribution of π_{metaR1} in Model 8 shows that more-hydrophobic substituents at the *meta* position of the anilino ring are favorable for enhanced GSK-3α inhibitory activity. Note that the most active compound among the whole series is **38**, with 3,5-dichloro substituents at R_1. Apparently the inherent hydrophobicity of the chlorine atom makes it a suitable *meta* substituent for better hydrophobic interactions with the active site of GSK-3α.

Model 9 was obtained by adding HA_R to Model 8, resulting from a stepwise attempt to improve the statistical quality. Model 9 is significantly better than Model 8. Models 10 and 11 included f_{ortho} and E^{s}_{orthoR}, respectively, to test for effects of *ortho* substituents as in Models 2 and 3, while also including π_{metaR1}. They each are slightly better than Model 9 and approximately equally good. Model 12 was developed by adding σ_{metaR} to Model 9. This resulted in a further small improvement in the statistical quality. Models 13 and 14 included f_{ortho} and E^{s}_{orthoR}, respectively, to test for effects of *ortho* substituents together with π_{metaR1} and σ_{metaR}. Model 14, the best model we found which includes all of **1**–**67**, has $r^2 = 0.83$ and $q^2 = 0.79$. The correlation between the observed and predicted GSK-3α inhibitory activity obtained from the best QSAR model 14 is shown in

Figure 1. Models 13a and 14a differed from Models 13 and 14, respectively, only by omitting **19** as an outlier. The reason for the outlying behavior of **19** is not immediately apparent. However **19** is the least active compound among the 3-anilino derivatives. The statistical quality of Models 13a and 14a is better than that of the corresponding models containing **19**. Amongst all the 2D-QSAR models, Models 13a and 14a have the highest squared correlation coefficient ($r^2 = 0.85$) as well as the highest internal predictivity ($q^2 = 0.81$).

Figure 2 summarizes our 2D-QSAR findings suggesting where functional groups having particular physicochemical properties may best improve GSK-3α activity. As we discussed above, activity is enhanced by hydrophobic substituents on the anilino ring. There is a preference for N–H over an *N*-methyl linker for the anilino ring. Of particular importance is that electron-withdrawing groups are favored at *ortho* and *meta* positions of the 4-phenyl ring. This is in good agreement with the most active compounds of the series which possess a 3-nitro (**38**, the most active compound with IC_{50} of 20 nM, and **54**, the next most active compound with IC_{50} of 26 nM) or 2-nitro (**51** with IC_{50} of 28 nM) group at R. The nitro group is strongly electron-withdrawing due to available resonance structures, whereas the chloro group is weakly electron-withdrawing due to inductive effects. If we compare to derivatives with chloro substitution at these positions, we see that compounds with nitro groups are more potent (compare **38** and **36**, IC_{50} of 20 and 58 nM, respectively; **54** and **52**, IC_{50} of 26 and 76 nM, respectively, for *meta* position and **51** versus **50**: IC_{50} of 28 and 74 nM, respectively, for *ortho* position).

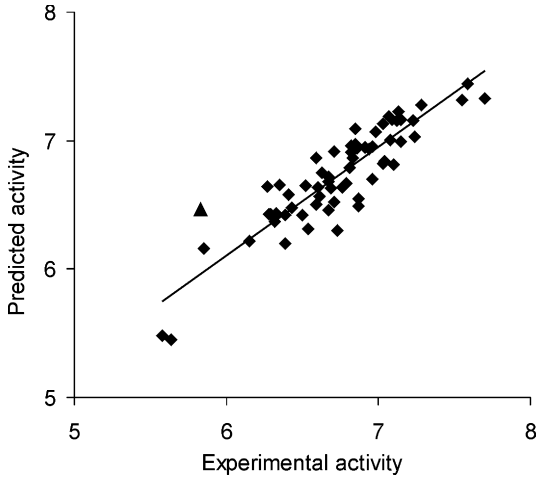

Figure 1. Correlation between the observed and predicted GSK-3α inhibitory activity from QSAR model 14 showing compound **19** as outlier (triangle).

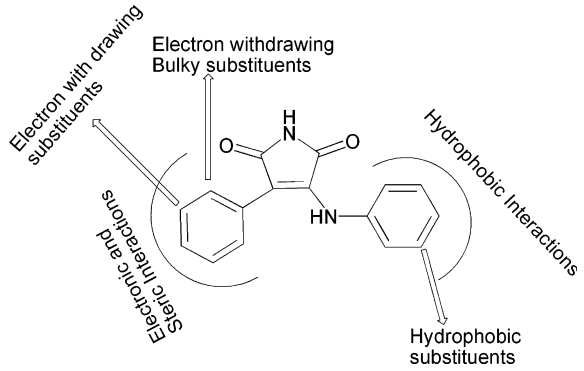

Figure 2. Proposed model based on 2D-QSAR analyses showing the nature of interactions and substitution requirements for effective binding of 3-anilino-4-phenylmaleimides with the GSK-3α isoform.

In 2D-QSAR it is important to verify the internal consistency of the models using q^2. One way to assess this is with the ratio $RQR = q^2/r^2$. Considering *RQR* for the 16 models listed in Table 4, it is pleasing that the lowest value is $RQR = 0.89$ for QSAR Model 1 and there is a gradual, roughly monotonic increase across the series to $RQR = 0.96$ for Models 13a and 14a. Thus the Hansch 2D-QSAR models we present are statistically robust.

2.3. Discussion of related work

The original authors who reported the data set, Smith et al.[21] had several comments analyzing the structure–activity relationship (SAR) of the series. Our Fujita–Ban analysis interpreted the contribution to activity of each substituent. Our work agrees with Smith et al.[21] (whose SAR analysis only commented on certain substituents) that on the 4-phenyl ring: 3-COOH; 4-Cl; and 4-OH in combination with 3-Cl or 3,5-di-Cl increase the activity, though from our analysis each of those groups helped to increase activity. Also for the 4-phenyl ring they noted that either electron-withdrawing or electron-donating groups were found on highly potent compounds, so they concluded that either electronic effects are relatively unimportant or that if they are important some of the compounds must adopt different binding modes. Our study gives more specific analysis and information about the electronic effects on this ring, showing that *ortho* and *meta* electron-withdrawing groups are important for enhanced activity.

Lescot et al.[39] in one of several available 3D-QSAR studies on GSK-3 inhibition, used CoMFA to study the influence of steric and electronic effects for the Smith et al.[21] inhibitory activity data set (which they called GSK-3β, not GSK-3α, data). They found the CoMFA steric field model was little different from the steric plus electrostatic model and hence ignored the importance of electronic effects on the activity. By contrast, in our work in addition to the steric factors emphasized by Lescot et al.[39] we also found electronic, hydrophobic, hydrogen bond acceptor, and some structural properties as important for activity enhancement. Our 2D findings are consistent with their steric contour plots from CoMFA, including the unfavorable effect of methyl substitution onto the aniline NH linker and the favorable effect of *para* bulky groups on the 3-anilino ring.

Katritzky et al. recently reported QSAR analysis of 277 GSK-3α, GSK-3β, and GSK-3α/β inhibitors.[42] Included

therein, they performed a multiple linear regression (MLR) analysis of 74 compounds from Smith et al.[21] We compared our models to theirs for the Smith et al. compounds, but it is important to note that our models did not include the 7 indolino maleimides. Interestingly, they also found **19** to be an outlier with overestimated predicted activity (plus they had one indolino outlier). In their MLR models for the maleimides, they picked the best 6 of 739 descriptors. In order of importance, based on highest *t*-score, they first had the Randić topological index, sometimes considered to be a measure of steric bulk for the whole ligand. Estrada interpreted the index to be the 'relative accessibility bond areas' available for interaction with the receptor.[46] As Randić himself has pointed out,[47] the interpretation of the Randić topological index is not simple and he suggested a more easily interpretable index would be one in which the functional groups at the edges of the ligand would receive extra weights.[47] Katritzky et al.[42] interpreted the importance of the Randić topological index by noting that the degree of branching and the bulk of the ligands are crucial for their activity. The importance that our 2D-QSAR analysis places on steric factors agrees with this. Next is the average Mulliken bond order for any bond involving H. This suffers from two problems: the Mulliken bond order is not always reliable (in fact there is no unique definition of the bond order using ab initio methods and a method such as the Mulliken one is very dependent on the basis set and level of theory, whereas the Mayer bond order[48] or natural bond order[49] may be more reliable). But another question is the correct interpretation of this index. Katritzky et al.[42] say it is related to the docking free energy or the hydrogen-bonding capability of the ligands, but it is certainly not a direct measure of these quantities. For our models, we found the hydrogen bonding descriptor HA to be important for activity. Other descriptors Katritzky et al. used were LUMO energy, HACA-2, charged surface area for atom N, and maximum coulombic interaction for bond C–C. Overall, they summarize the interaction as 'charge-related' or electrostatic, though they found their MLR descriptors were difficult to interpret directly.[42] In our Hansch 2D-QSAR approach, we have focused on descriptors that are widely used by QSAR researchers and easier to interpret than those used by Katritzky et al.[42] We were able to describe the nature of the interactions between the ligands and the target enzyme with the help of the descriptors we used (cf. Fig. 2).

3. Conclusion

GSK-3 inhibition is an attractive target identified to be useful in the treatment of diseases such as diabetes, Alzheimer's disease, stroke, and bipolar disorders. Due to the more promising role of the α isoform of this enzyme, we have explored the nature of interaction of ligands toward this isoform. The limited 3D structural information on this novel target (GSK-3α) hampers structure based drug design of this isoform in designing novel congeners. Reported herein is our 2D-QSAR approach, using Fujita–Ban/Hansch QSAR investigations on reported 3-anilino and 3-*N*-methylanilino-4-phenylmaleimides to gain insights about GSK-3α enzyme inhibition. Fujita–Ban analysis of 3-anilino-4-phenylmaleimides revealed that certain structural features such as Cl, OCH_3, and NO_2 mono substitution at any position around the 4-phenyl ring were favorable for GSK-3α inhibition. Substituents at the 3-anilino ring such as 3-Cl, 4-Cl, 5-Cl, 3-COOH, 4-OH, and 4-SCH_3 were positively and 3-OH was negatively correlated with GSK-3α inhibitory activity.

Through Hansch QSAR analyses, we found that the GSK-3α inhibitory activity was enhanced by:

1. Electron-withdrawing, bulky *ortho* substituents at 4-phenyl ring
2. 4-chloro substitution around anilino ring
3. 3-anilino rather than 3-*N*-methylanilino derivatives
4. Hydrophobic *meta* substituents on the anilino ring

Overall, QSAR models 13a and 14a suggest electronic and steric effects at the 4-phenyl ring and hydrophobic effects at the 3-anilino or 3-*N*-methylanilino ring are crucial. Our 2D-model (Fig. 2) illustrates these effects which are essential for binding of the maleimides to the GSK-3α enzyme. Our analysis has provided key information regarding ligand–target interactions which we believe will help medicinal chemists to design more potent GSK-3α inhibitors.

4. Materials and methods

The reported series of 4-phenylmaleimides[21] includes 64 compounds with 3-anilino, 4 compounds with 3-*N*-methylanilino, and 7 compounds with 3-indolino groups. Out of these, only the 3-anilino and 3-*N*-methylanilino compounds were considered for our 2D-QSAR studies since they have a similar backbone. Also, one 3-*N*-methylanilino derivative was not included in the present study as no well-defined biological activity data were reported. Among the 3-anilino derivatives, major substitution changes were reported around the 4-phenyl ring (with mono-substituents) and around the 3-anilino ring (with mono- and di-substituents). We converted the experimental activities against hGSK-3α (which Smith et al. obtained for each compound using a 4-parameter model)[21] from IC_{50} in nM to pIC_{50}. The 67 compounds used for the analysis along with their observed and converted activity are listed in Table 1. QSAR models were evaluated using statistical parameters such as the correlation coefficient (r) or coefficient of determination (r^2), standard error of estimate (s), Fischer F-value, and Student's t-distribution (used to assess the significance of the individual regression terms).

2D-QSAR models were constructed using the data set of 67 compounds.[21] Linear regression analysis was performed using Systat 11.[50] We used two types of standard descriptors, indicator variables and physicochemical constants. An indicator variable designated as I with a relevant subscript was set to 1 if a particular substituent or chemical feature is present and to 0 if absent. Classic Hansch 2D-QSAR physicochemical

constants—hydrophobic (π), electronic (σ), including resonance effect (R) or field/inductive effect (f), and molar refractivity (MR)—were taken from the literature.[51] In general, electronic effects can be represented as a combination of a field (inductive) effect, f, and a resonance effect, R. (This f, which reflects the electronic properties of the substituents, is different from the F statistic, which is the Fischer test for significance of QSAR models, so we use lowercase f for it.) The substituent hydrophobicity constant (π_X) for any substituent X is calculated according to the equation, $\pi_X = \log P_X - \log P_H$, where P_X and P_H are the experimental partition coefficients of the reference compound with and without substituent, respectively. The Hammett electronic parameter (σ) is calculated based on the influence of substituent X on the ionization of benzoic acid. The molar refractivity (MR) is roughly a measure of the volume and polarizability of an atom or group of atoms and is calculated using the Lorentz–Lorenz equation. A correlation matrix was used to correlate the biological activity with the various physicochemical and structural predictor variables. Forward-stepping regression was used to build each QSAR model. This method initially generates a QSAR model containing only one variable, chosen to be the one with the highest t-statistic; subsequent variables are added based on their relative importance as determined by t-statistics. For example, though we considered MR as a descriptor, it was determined to be relatively unimportant and hence is not included in any of the models reported in this work. Some descriptors were added or deleted to get more insight about the nature of interactions of these ligands with GSK-3α. Pairs of descriptors with intercorrelation >0.5 were not included in the same QSAR model. A data point was considered an outlier when its residual value exceeded twice the standard error of estimate of the model. Self-consistency of the derived models was ensured using the leave-one-out (loo) process. The predictability of each model was assessed using *cross-validated* r^2, usually called q^2.

Acknowledgment

Funding from University of Mississippi, including from its Faculty Research Program, from NSF EPS-0556308 and from CDC Grants U01/CI000211-02 and U50/CCU423310-02 as well as Laboratory for Applied Drug Design and Synthesis facilities are greatly appreciated. This investigation was conducted in a facility constructed with support from research facilities improvement program C06 RR-14503-01 from the NIH National Center for Research Resources. Thanks to Pankaj R. Daga for helpful discussions and Zhi Bie for assistance.

Supplementary data

Supplementary data associated with this article consisting of the Fujita–Ban matrix and Hansch descriptor intercorrelation matrices can be found, in the online version, at doi:10.1016/j.bmc.2006.09.021.

References and notes

1. Ali, A.; Hoeflich, K. P.; Woodgett, J. R. *Chem. Rev.* **2001**, *101*, 2527.
2. Hanks, S. K.; Hunter, T. *FASEB J.* **1995**, *9*, 576.
3. Embi, N.; Rylatt, D. B.; Cohen, P. *Eur. J. Biochem.* **1980**, *107*, 519.
4. Eldar-Finkelman, H.; Schreyer, S. A.; Shinohara, M. M.; LeBoeuf, R. C.; Krebs, E. G. *Diabetes* **1999**, *48*, 1.
5. Nikoulina, S. E.; Ciaraldi, T. P.; Mudaliar, S.; Carter, L.; Johnson, K.; Henry, R. R. *Diabetes* **2002**, *51*, 2190.
6. Ciaraldi, T. P.; Nikoulina, S. E.; Henry, R. R. *J. Diabetes Complications* **2002**, *16*, 69.
7. Sarabu, R.; Tilley, J. *Annu. Rep. Med. Chem.* **2004**, *39*, 41.
8. Wagman, A. S.; Johnson, K. W.; Bussiere, D. E. *Curr. Pharm. Des.* **2004**, *10*, 1105.
9. Phiel, C. J.; Wilson, C. A.; Lee, V. M.-Y.; Klein, P. S. *Nature* **2003**, *423*, 435.
10. Alvarez, G.; Munoz-Montano, J. R.; Satrustegui, J.; Avila, J.; Bogonez, E.; Diaz-Nido, J. *Bipolar Disord.* **2002**, *4*, 153.
11. Bhat, R. V.; Budd Haeberlein, S. L.; Avila, J. *J. Neurochem.* **2004**, *89*, 1313.
12. Bhat, R. V.; Budd, S. L. *Neurosignals* **2002**, *11*, 251.
13. Murphy, E.; Steenbergen, C. *Expert Opin. Ther. Targets* **2005**, *9*, 447.
14. Manoukian, A. S.; Woodgett, J. R. *Adv. Cancer Res.* **2002**, *84*, 203.
15. Gould, T. D.; Zarate, C. A.; Manji, H. K. *J. Clin. Psychiatry* **2004**, *65*, 10.
16. Droucheau, E.; Primot, A.; Thomas, V.; Mattei, D.; Knockaert, M.; Richardson, C.; Sallicandro, P.; Alano, P.; Jafarshad, A.; Baratte, B.; Kunick, C.; Parzy, D.; Pearl, L.; Doerig, C.; Meijer, L. *Biochim. Biophys. Acta* **2004**, *1697*, 181.
17. Woodgett, J. R. *EMBO J.* **1990**, *9*, 2431.
18. Mukai, F.; Ishiguro, K.; Sano, Y.; Fujita, S. C. *J. Neurochem.* **2002**, *81*, 1073.
19. Alonso, M.; Martinez, V. *Curr. Med. Chem.* **2004**, *11*, 755.
20. Coghlan, M. P.; Culbert, A. A.; Cross, D. A.; Corcoran, S. L.; Yates, J. W.; Pearce, N. J.; Rausch, O. L.; Murphy, G. J.; Carter, P. S.; Roxbee, C. L.; Mills, D.; Brown, M. J.; Haigh, D.; Ward, R. W.; Smith, D. G.; Murray, K. J.; Reith, A. D.; Holder, J. C. *Chem. Biol.* **2000**, *7*, 793.
21. Smith, D. G.; Buffet, M.; Fenwick, A. E.; Haigh, D.; Ife, R. J.; Saunders, M.; Slingsby, B. P.; Stacey, R.; Ward, R. W. *Bioorg. Med. Chem. Lett.* **2001**, *11*, 635.
22. Eickholt, B. J.; Walsh, F. S.; Doherty, P. *J. Cell. Biol.* **2002**, *157*, 211.
23. Witherington, J.; Bordas, V.; Garland, S. L.; Hickey, D. M.; Ife, R. J.; Liddle, J.; Saunders, M.; Smith, D. G.; Ward, R. W. *Bioorg. Med. Chem. Lett.* **2003**, *13*, 1577.
24. Witherington, J.; Bordas, V.; Haigh, D.; Hickey, D. M.; Ife, R. J.; Rawlings, A. D.; Slingsby, B. P.; Smith, D. G.; Ward, R. W. *Bioorg. Med. Chem. Lett.* **2003**, *13*, 1581.
25. Witherington, J.; Bordas, V.; Gaiba, A.; Garton, N. S.; Naylor, A.; Rawlings, A. D.; Slingsby, B. P.; Smith, D. G.; Takle, A. K.; Ward, R. W. *Bioorg. Med. Chem. Lett.* **2003**, *13*, 3055.
26. Witherington, J.; Bordas, V.; Gaiba, A.; Naylor, A.; Rawlings, A. D.; Slingsby, B. P.; Smith, D. G.; Takle, A. K.; Ward, R. W. *Bioorg. Med. Chem. Lett.* **2003**, *13*, 3059.
27. Ring, D. B.; Johnson, K. W.; Henriksen, E. J.; Nuss, J. M.; Goff, D.; Kinnick, T. R.; Ma, S. T.; Reeder, J. W.; Samuels, I.; Slabiak, T.; Wagman, A. S.; Hammond, M. E.; Harrison, S. D. *Diabetes* **2003**, *52*, 588.
28. Bhat, R.; Xue, Y.; Berg, S.; Hellberg, S.; Ormo, M.; Nilsson, Y.; Radesater, A. C.; Jerning, E.; Markgren, P.

O.; Borgegard, T.; Nylof, M.; Gimenez-Cassina, A.; Hernandez, F.; Lucas, J. J.; Diaz-Nido, J.; Avila, J. *J. Biol. Chem.* **2003**, *278*, 45937.
29. Kuo, G. H.; Prouty, C.; DeAngelis, A.; Shen, L.; O'Neill, D. J.; Shah, C.; Connolly, P. J.; Murray, W. V.; Conway, B. R.; Cheung, P.; Westover, L.; Xu, J. Z.; Look, R. A.; Demarest, K. T.; Emanuel, S.; Middleton, S. A.; Jolliffe, L.; Beavers, M. P.; Chen, X. *J. Med. Chem.* **2003**, *46*, 4021.
30. Martinez, A.; Alonso, M.; Castro, A.; Dorronsoro, I.; Gelpi, J. L.; Luque, F. J.; Perez, C.; Moreno, F. J. *J. Med. Chem.* **2005**, *48*, 7103.
31. Hansch, C.; Fujita, T. *J. Am. Chem. Soc.* **1964**, *86*, 1616.
32. Garg, R.; Kurup, A.; Mekapati, S. B.; Hansch, C. *Chem. Rev.* **2003**, *103*, 703.
33. Dajani, R.; Fraser, E.; Roe, S. M.; Young, N.; Good, V.; Dale, T. C.; Pearl, L. H. *Cell* **2001**, *105*, 721.
34. ter Haar, E.; Coll, J. T.; Austen, D. A.; Hsiao, H.-M.; Swenson, L.; Jain, J. *Nat. Struct. Biol* **2001**, *8*, 593.
35. Fujita, T.; Ban, T. *J. Med. Chem.* **1971**, *14*, 148.
36. Cramer, R. D., III; Patterson, D. E.; Bunce, J. D. *J. Am. Chem. Soc.* **1988**, *110*, 5959.
37. Klebe, G.; Abraham, U.; Mietzner, T. *J. Med. Chem.* **1994**, *37*, 4130.
38. Zeng, M.; Jiang, Y.; Zhang, B.; Zheng, K.; Zhang, N.; Yu, Q. *Bioorg. Med. Chem. Lett.* **2005**, *15*, 395.
39. Lescot, E.; Bureau, R.; Sopkova-de Oliveira Santos, J.; Rochais, C.; Lisowski, V.; Lancelot, J. C.; Rault, S. *J. Chem. Inf. Model.* **2005**, *45*, 708.
40. Zhang, N.; Jiang, Y.; Zou, J.; Zhang, B.; Jin, H.; Wang, Y.; Yu, Q. *Eur. J. Med. Chem.* **2006**, *41*, 373.
41. Xiao, J.; Guo, Z.; Guo, Y.; Chu, F.; Sun, P. *Protein Eng. Des. Sel.* **2006**, *19*, 47.
42. Katritzky, A. R.; Pacureanu, L. M.; Dobchev, D. A.; Fara, D. C.; Duchowicz, P. R.; Karelson, M. *Bioorg. Med. Chem.* **2006**, *14*, 4987.
43. Patel, D. S.; Bharatam, P. V. *J. Comput. Aided Mol. Des.* **2006**, *20*, 55.
44. Fujita, T.; Nishioka, T. *Prog. Phys. Org. Chem.* **1976**, *12*, 49.
45. Hansch, C. *Il Farmaco* **2003**, *58*, 625.
46. Randić, M.; Zupan, J. *J. Chem. Inf. Comput. Sci.* **2001**, *41*, 550.
47. Estrada, E. *Internet Electron. J. Mol. Des.* **2002**, *1*, 360.
48. Doerksen, R. J.; Thakkar, A. J. *Int. J. Quantum Chem.* **2002**, *90*, 534.
49. Weinhold, F.; Landis, C. R. *Valency and Bonding: A Natural Bond Orbital Donor–Acceptor Perspective*; Cambridge University Press, 2003.
50. Systat 11, Systat Software Inc., 2002.
51. Hansch, C.; Leo, A. *Substituent Constants for Correlation Analysis in Chemistry and Biology*, John Wiley and Sons, New York, 1979, p. 48.